C.P. No. 802

C.P. No. 802


MINISTRY OF AVIATION

*AERONAUTICAL RESEARCH COUNCIL*

*CURRENT PAPERS*

# Wind Tunnel Measurements of the Far-Field Pressures due to some Lifting, Slender Delta Wings

*by*

*T. A. Cook*

LONDON: HER MAJESTY'S STATIONERY OFFICE

1965

PRICE 6*s* 6*d* NET

U.D.C. No. 533.693.3 : 533.6.048.2 : 533.6.011.5

C.P. No. 802

August, 1964

# WIND TUNNEL MEASUREMENTS OF THE FAR-FIELD PRESSURES DUE TO SOME LIFTING, SLENDER DELTA WINGS

by

T. A. Cook

---

## SUMMARY

Measurements have been made of the pressure field in the plane of symmetry of each of three slender delta wings of unit aspect ratio, at a distance of 12 model lengths from each model and at a Mach number of 1.80. One model was uncambered while the others were cambered to have attached flow at their leading edges at $C_L = 0.1$: the cambered models had different lengthwise lift distributions.

Estimates of the front shock wave strengths of the models made using Whitham's theory were found to be in good agreement with the measured values, though estimates of lift effects seemed a little low. An estimate of the complete pressure signature of a model at zero lift agreed well with measurements.

---

Replaces R.A.E. Tech. Note No. Aero 2976 - A.R.C. 26436

## CONTENTS


| | | Page |
|---|---|---|
| 1 | INTRODUCTION | 4 |
| 2 | THE MODELS AND SUPPORT SYSTEM | 4 |
| 3 | TEST TECHNIQUE | 5 |
| 4 | DISCUSSION OF RESULTS | 5 |
| 5 | CONCLUSIONS | 7 |
| SYMBOLS | | 8 |
| REFERENCES | | 9 |
| APPENDIX - Theoretical Estimates | | 10 to 14 |
| ILLUSTRATIONS - Figs. 1-17 | | - |
| DETACHABLE ABSTRACT CARDS | | - |


## ILLUSTRATIONS


| | Fig. |
|---|---|
| Details of models A, B and C | 1 |
| Lengthwise distribution of cross-sectional area of the models | 2 |
| Lengthwise distribution of lift on the models at $C_L = 0.1$ | 3 |
| Sketch of model support and actuating system | 4 |
| Photograph of a model on the support system | 5 |
| Arrangement of model and probe in the wind tunnel | 6 |
| Pressure measurements for Model A | 7 |
| Pressure measurements for Model B | 8 |
| Pressure measurements for Model C | 9 |
| Comparison of experimental and estimated pressure signatures for Model A at $C_L = 0$ | 10 |
| Comparison of pressure measurements for Models A and B | 11 |

## ILLUSTRATIONS (Cont'd)


| | Fig. |
|---|---|
| Measured front shock strengths of Models A, B and C | 12 |
| Estimated front shock strengths of Models A, B and C | 13 |
| Comparison of measured and estimated front shock strengths for models with conical lift distribution | 14 |
| Comparison of measured and estimated front shock strengths for model with non-conical lift distribution | 15 |
| Typical F-functions used to estimate front shock wave strengths | 16 |
| Complete F-function for Models A and B at zero $C_L$ | 17 |

## 1 INTRODUCTION

Since the likely effects of the so-called 'sonic boom' due to proposed supersonic transport aircraft are of sufficient importance to influence the use and flight plan of such an aircraft (e.g. Ref.1), it is essential to be able to predict pressures in the far field of such an aircraft accurately. Methods of estimation are based on a theory, which is essentially a modified linearised theory, originally propounded by Whitham[2] and further developed by Whitham[3] and Walkden[4]. Since current designs for supersonic transports involve slender wings with leading edge separations occurring at all except one particular incidence, it was thought necessary to check Whitham's theory for this type of flow. A possibility existed that the strength of the front shock wave below an aircraft might differ from that predicted by theory when the flow was separated.

Some wind tunnel measurements of far-field pressures have been made by Carlson[5], principally those produced by non-lifting bodies, though some work on the effect of angle of incidence is included. Other comparisons between theory and experiment have been made using full-scale aircraft (e.g. Refs.6 and 7). All measurements have shown good agreement with estimates, but have not included the case of a slender aircraft. The present wind tunnel measurements were intended to provide a check for this case.

The tests were made in the 8 ft x 8 ft tunnel at R.A.E. Bedford during August, 1961.

## 2 THE MODELS AND SUPPORT SYSTEM

Three models (Fig.1) were used for the tests. All were delta wings of unit aspect ratio with centre-line chord lengths of 6 inches. The lengthwise distribution of cross-sectional area (Fig.2) was the same for each model and was a Lord V distribution with a maximum thickness-chord ratio of 8.43% at the centre-line.

The three models have been designated A, B and C. Model A was uncambered with rhombic spanwise sections while the other two models were cambered versions of A. Model B was cambered conically by Brebner's method: the camber used is specified in Ref.8 by the parameter n = 2, with the camber shoulder-line at 75% of the local semi-span, and was designed to give attached flow at the leading edge at $C_L$ = 0.1 and M = 1.0. Model C was cambered and twisted by Roper's method, being in fact Wing 3 of Ref.9, which was designed to have attached flow at $C_L$ = 0.1 and M = 1.56. Models A and B had theoretically linear lengthwise load distributions while Model C had a non-linear distribution, (Fig.3).

A sketch of the model support system is shown in Fig.4 and a photograph in Fig.5. By means of the actuating systems the model could be pitched through an angle of over 5° and traversed in the streamwise direction a total distance of about 8 inches. The centre of rotation in pitch was at the centre of area of Models A and B; in the case of Model C a support strut 3 inches longer was used with a consequent displacement of the model ahead of the centre of rotation.

## 3 TEST TECHNIQUE

The arrangement of the model and static probe in the tunnel is shown in Fig.6. The probe could be traversed in the streamwise direction at a distance of 12 inches from the tunnel wall opposite that on which each model was mounted. All measurements were thus made in a streamwise plane through the model centre-line and normal to the plane of the wing, and at a distance r, normal to the free-stream direction, of 12.0 model lengths from each of Models A and B and 11.85 model lengths from Model C, (due to the longer support). Measurements of the bow shock wave strength for Model C were corrected for this small difference in distance by assuming the shock strength to be proportional to $r^{-3/4}$, i.e. the theoretical asymptotic variation for large r.

Probe static measurements, p, were referenced to free-stream static pressure, $p_o$, and the ratio $p-p_o/p_o$ obtained. In the tunnel free-stream (i.e. with no gradients or disturbances present), this ratio was found to be accurate to within ±0.0004. Errors due to interactions between shock waves and the probe boundary layer and to vibrations of the model and shock wave, etc., are discussed in Section 4.

The procedure adopted in surveying the model pressure field was to traverse the model streamwise with the probe in a pre-selected position. It was not possible to explore a complete pressure signature with a single probe position because of the limited range of model movement: consequently in the cases where the full pressure signature has been obtained two probe positions have been set up. In most cases, however, only the region of the bow shock wave was surveyed.

Measurements were made for each model at a Mach number of 1.80 and a Reynolds' number of $4.25 \times 10^6$ per foot at several angles of incidence. The lift coefficient corresponding to each incidence angle was determined in the case of Models A and B from force measurements made on larger models in the 8 ft x 8 ft tunnel[10]. In the case of Model C, the lift coefficient at the design attitude (i.e. at the incidence intended to give attached flow at M = 1.56) was calculated by linearised theory[9,11] to be 0.098 at M = 1.80. The lift curve slope was taken as the mean of those measured on Models A and B over a 5° incidence range, (these mean slopes differed by less than 1% and represented the variation of $C_L$ with $\alpha$ with negligible error over this range).

## 4 DISCUSSION OF RESULTS

Plots of the basic measurements made are presented in Figs.7, 8 and 9. In these figures the origin of streamwise distance is arbitrary, being merely the extreme downstream position of each model when the front section of the pressure signature was being explored. The origin of the pressure co-ordinate $(p-p_o)/p_o$ is the mean of values obtained in the free stream ahead of the pressure field of each model.

The blunting and rounding of the pressure profiles in the neighbourhood of shock waves is probably due to a combination of the following causes:-

(1) shock wave - boundary layer interactions on the static probe;

(2) vibrations of the model and/or probe;

(3) tunnel free-stream turbulence, resulting in vibration of the shock wave over the probe.

If it can be assumed that the blunting process is due only to limitations of the measuring technique and that elimination of these would result in a 'sharp' bow shock wave being obtained, then the blunting effect can be approximately corrected for as shown in Fig.7. The pressure rise between the rear and front shock waves has been continued forward and terminated in a sharp bow wave, the position of which has been chosen by satisfying the condition $I_1 = I_2$. (This condition is obtained if vibration errors are assumed to predominate and the static pressure measured is a simple mean of the variation during one oscillation.) The profiles in the region of the front shock waves obtained using this correction method are shown as broken lines in Figs.7 to 9.

In Fig.10 the pressure signature of Model A at $C_L = 0$ is compared with an estimate made using the method outlined in the Appendix. In order to superimpose the estimated signature on the experimental results, it has been assumed that the theoretical front shock wave coincided with the corrected experimental front shock wave in streamwise position. On this basis Fig.10 shows good agreement between theory and experiment over all parts of the pressure signature, in spite of the simple wake model assumed and neglect of the model support in the estimates.

The front parts of the pressure signatures of Models A and B are compared at identical lift coefficients in Fig.11. The small differences observed are of about the same magnitude as the possible error; however if camber does contribute to them, then the comparison would be expected to be even better at greater distances from the models, when the asymptotic N-type pressure signature is approached.

Measured front shock wave strengths for the three models (using the corrected pressure profiles) have been plotted against $C_L$, and are compared with each other in Fig.12 and with theory in Figs.14 and 15. Fig.13 compares the estimated values (see Appendix). Fig.12 shows no significant difference between the front shock wave strengths of Models A and B, the inference being that the shock wave strength is independent of the $C_L$ value at which leading edge flow is attached. Fig.14 shows that the estimates are in good agreement with the mean experimental results for Models A and B, though the theory indicates a rather smaller increase of shock wave strength with lift coefficient than that measured. It should be noted that, since the experimental results for Models A and B agree with each other, this disagreement cannot be ascribed to the occurrence of separated flows.

Estimates indicate (Fig.13) that, as a result of the different lengthwise loading of Model C compared with Models A and B, Model C should have a weaker front shock wave over the $C_L$ range covered in the experiment: measurements show,

however, that the reverse is the case (Fig.12). There is thus for Model C rather poorer agreement between estimate and experiment (Fig.15) than that obtained for Models A and B. This discrepancy might arise if the theoretical lift distribution assumed in deriving the F-function and $C_L$ v. $\alpha$ relationship for Model C were not achieved in practice*. As in the case of Models A and B, a smaller effect due to lift is obtained theoretically than that obtained experimentally. (A similar effect is to be expected for all three models since, according to linearised theory, the incremental distribution of lift due to incidence is independent of camber design.)

## 5 CONCLUSIONS

A wind tunnel technique for measuring the pressures at a large distance from small models in supersonic flow has been described, and used to explore the far pressure fields of three lifting, slender delta wings at a distance of 12 model lengths and a Mach number of 1.80. Allowance has been made for deficiencies in the technique which result in weakening and thickening of measured shock waves. The results have been compared with estimates made using Whitham's theory and the following conclusions reached:-

(1) Theory agreed well with measurements of the complete pressure signature for an uncambered model at zero lift.

(2) There was good agreement between the front shock wave strengths of two models, both having linear lengthwise lift distributions but different attachment lift coefficients. Theory also agreed well with both, though the predicted variation of front shock wave strength with lift coefficient was somewhat lower than that measured: the effect was, however, relatively small and of the same size as the experimental error.

(3) Theory agreed less well in the case of the front shock waves produced by a cambered model with a non-linear lengthwise lift distribution. Again the estimated increase with lift was rather less than that measured.

These results indicate that far-field pressures, in particular front shock wave strengths, can be predicted fairly accurately in the case of a slender wing irrespective of the lift coefficient at which leading edge flow is attached. The greater apparent discrepancy between theory and measurement in the case of a wing with a non-linear lengthwise distribution of lift could probably be overcome if the lift distribution were accurately known. It is possible however that, for an aircraft flying at high altitudes, when the lift contribution to the sonic boom is important, the strength of the shock wave on the ground may be underestimated by theory.

---

*The camber of Model C was designed to effect a departure from conical loading (in addition to attached flow at a given $C_L$), and therefore the estimates depend on the extent to which the camber design is effective. The theoretical conical loadings on Models A and B are unmodified by camber and are thus more likely to be achieved in practice.

## SYMBOLS

| | |
|---|---|
| $M$ | Mach number |
| $C_L$ | Lift coefficient = lift force/kinetic pressure × model plan area |
| $p$ | static pressure |
| $p_o$ | free-stream static pressure |
| $\Delta p$ | change in static pressure associated with a shock wave |

$\ell(t,s)$ local loading coefficient $= \dfrac{(p)_{\text{lower surface}} - (p)_{\text{upper surface}}}{\text{kinetic pressure}}$

$$L(t) = \int_{-t/4}^{t/4} \ell(t,s)\, ds, \text{ (in model length units)}$$

$t,s,r$ co-ordinate system with origin at model apex: t and s are along and perpendicular to model longitudinal axis respectively, in the plane of the model: r is parallel to the lift vector, but in the opposite sense. The unit of length is one model length (6 inches)

$y$ lengthwise parameter defined by equation (4) of Appendix: unit of length is one model length

---

## REFERENCES


| No. | Author | Title, etc. |
|---|---|---|
| 1 | Lina, L.J.<br>Maglieri, D.J.<br>Hubbard, H.H. | Supersonic transports - noise aspect with emphasis on sonic boom.<br>S.M.F. Fund Paper No. FF-26<br>Inst. of Aero Sciences 28th Annual Meeting<br>January, 1960. |
| 2 | Whitham, G.B. | The flow pattern of a supersonic projectile.<br>Communications on Pure and Applied Maths. Vol. V, No.3, pp.301-348. August, 1952. |
| 3 | Whitham, G.B. | On the propagation of weak shock waves.<br>Journal of Fluid Mechanics, Vol.I, p.290 ff. 1956. |

## REFERENCES (Cont'd)


| No. | Author | Title, etc. |
|---|---|---|
| 4 | Walkden, F. | The shock pattern of a wing-body combination far from the flight path. Aero. Quarterly, Vol.IX, p.180. 1958. |
| 5 | Carlson, H.W. | An investigation of some aspects of the sonic boom by means of wind tunnel measurements of pressures about several bodies at a Mach number of 2.01. N.A.S.A. T.N. D-161. December, 1959. |
| 6 | Smith, H.J. | Experimental and calculated flow fields produced by airplanes flying at supersonic speeds. N.A.S.A. T.N. D-621. November, 1960. |
| 7 | Maglieri, D.J. Hubbard, H.H. | Ground measurements of the shock wave noise from supersonic bomber airplanes in the altitude range from 30,000 to 50,000 ft. N.A.S.A. T.N. D-880 A.R.C. 23,204. July, 1961. |
| 8 | Brebner, G.G. | Some simple conical camber shapes to produce low lift-dependent drag on a slender delta wing. A.R.C. C.P. 426. September, 1957 |
| 9 | Roper, G.M. | Use of camber and twist to produce low drag delta or swept-back wings, without leading edge singularities, at supersonic speeds. A.R.C. R. & M. 3196. December 1958. |
| 10 | Philpott, D.R. Ormerod, A.O. | Wind tunnel tests on a cambered delta wing of unit aspect ratio at Mach numbers between 1.4 and 2.4. Unpublished N.P.L. Report. |
| 11 | Roper, G.M. | Drag reduction of thin wings at supersonic speeds, by the use of camber and twist. A.R.C. R. & M. 3132. July, 1957. |

## APPENDIX

## THEORETICAL ESTIMATES

Estimates of the front shock strengths and complete pressure signatures of the models tested were made using Whitham's theory of far-field pressures[2,3,4]. The following is the application of the theory to the present case: allowance is made for boundary layer thickness on the model and for a simple wake, but none is made for the presence of the model support. Calculations are restricted to the case of the pressure field in a plane parallel to the free-stream and normal to the plane of the wing, through the model centre line. Only the field below the wing is considered.

### THE F-FUNCTIONS

Far-field pressure signatures are determined in terms of the F-function. Consider a lifting, slender wing with lengthwise distribution of cross-sectional area $S_A(t)$, an additional area distribution $S_B(t)$ due to boundary layer thickness and wake, and lengthwise lift distribution $L(t)$. The unit of length is taken to be the length of each model, i.e. 6 inches. If $S(t) = S_A(t) + S_B(t)$, and $S'(t)$ and $L(t)$ are continuous functions of t, then the F-function is defined as:

$$F(y) = F_V(y) + F_L(y) \qquad (1)$$

where

$$F_V(y) = \frac{1}{2\pi} \int_0^y \frac{d\,S'(t)}{\sqrt{y - t}} \qquad (2)$$

and

$$F_L(y) = \frac{\beta}{4\pi} \int_0^y \frac{d\,L(t)}{\sqrt{y - t}} \qquad (3)$$

y is defined by the equation,

$$t = \beta r - k\,F(y)\,r^{\frac{1}{2}} + y \qquad (4)$$

in which $k = (\gamma+1)M^4/\sqrt{2}\,\beta^{3/2}$, $\beta = \sqrt{M^2 - 1}$, and r is a distance co-ordinate parallel to the direction of the lift force but opposite in sense: $\gamma$ is taken to be 1.4. When discontinuities occur in $S'(t)$ and $L(t)$, equations (2) and (3) cannot be used in the vicinity of such discontinuities: in Ref.2 Whitham derives an expression for the case of a body of revolution which can have discontinuities in $S'(t)$. However, although equation (2) has been shown to be the same for a slender wing as for a body of revolution, the use of discontinuity formulae derived for a body of revolution does not appear to have been

similarly mathematically justified. Thus, in the present case, a boundary layer-wake system has been chosen to avoid a discontinuity in $S'(t)$ at the wing trailing edge, although there is a discontinuity in $S'_A(t)$ at this position.

The present models have an area distribution given by:

$$S_A(t) = 0.03941\ t(1-t)[1-(1-t)^4] .$$

The boundary layer contribution to volume has been estimated assuming a laminar, compressible, 'flat plate' development along the model centre line given by

$$\delta^* = \frac{3.26}{\sqrt{R_t}} \times t ,$$

where $\delta^*$ is displacement thickness and $R_t$ is Reynolds' number based on the distance t. The thickness is assumed to vary as the square root of spanwise distance so that,

$$S_B(t) = 0.00149\ t^{3/2} ;$$

i.e.

$$S(t) = 0.03941\ t(1-t)[1-(1-t)^4] + 0.00149\ t^{3/2} .$$

This distribution has been applied for $t \leq 0.95$, while for $t \geq 1.05$ a wake of constant cross-sectional area has been assumed equal to the boundary layer area indicated for $t = 1.0$ by the above relation for $S_B(t)$, i.e. $S(t) = 0.00149$, $t \geq 1.05$. Within the region $0.95 \leq t \leq 1.05$ a polynomial expression for $S(t)$ has been derived which has the same values of $S(t)$ and $S'(t)$ at $t = 0.95$ and 1.05 as the distributions for $t \leq 0.95$ and $t \geq 1.05$ respectively. It was found,

$$S(t) = -0.00455 + 0.2221\ t - 0.4066\ t^2 + 0.1910\ t^3 ,$$
$$0.95 \leq t \leq 1.05 .$$

$S(t)$ and $S_A(t)$ are shown in Fig.2.

The lift distribution for Models A and B is assumed to be given by:

$$L(t) = \tfrac{1}{2} C_L\ t ,$$

and for Model C, using Ref.9,

$$L(t) = \frac{\pi}{10} t^3 (a - bt + ct^2) + \frac{1}{2} (C_L - 0.1)\, t ,$$

where $a = 3.8861$ , $b = 8.1598$ , $c = 4.4400$ .

The lengthwise lift distributions for all three models are shown in Fig.3 for $C_L = 0.1$.

The F-functions for the models were thus derived using the above distributions and equations (2) and (3).

For $y \leq 0.95$,

$$F_V(y) = \frac{0.31528}{\pi} y^{\frac{1}{2}} \left\{1 - 5y + 8y^2 - \frac{40}{7} + \frac{32}{21} y^4\right\} + 0.00056 .$$

For $0.95 \leq y \leq 1.05$,

$$F_V(y) = E + \frac{1}{\pi}\sqrt{y - 0.95}\ \{0.764\, y - 0.4503\} .$$

For $y \geq 1.05$,

$$F_V(y) = E + \frac{1}{\pi}\sqrt{y-0.95}\ \{0.764\, y - 0.4503\} - \frac{1}{\pi}\sqrt{y-1.05}\ \{0.764\, y - 0.4121\}$$

Here,

$$E = \frac{0.07882}{\pi}\sqrt{y}\left\{A + By + Cy^2 + Dy^3 + \frac{5}{3} y^4\right\}$$

$$- \frac{0.07882}{\pi}\sqrt{y-0.95}\left\{A + B(y-0.95) + C(y-0.95)^2 + D(y-0.95)^3 + \frac{5}{3}(y-0.95)^4\right\}$$

$$+ \frac{0.00112}{\pi} \arcsin\sqrt{\frac{0.95}{y}} ,$$

where $A = 4 - 30y + 60y^2 - 50y^3 + 15y^4$ , $B = 10 - 40y + 50y^2 - 20y^3$ ,

$C = 12 - 30y + 18y^2$ , $D = 7.1429 - 8.5714y$ .

$F_V(y)$, which is identical to $F(y)$ for Models A and B at zero lift, is shown in Fig.17.

For Models A and B,

$$F_L(y) = 0.1190\, C_L\, y^{\frac{1}{2}} \quad ;$$

and for Model C,

$$F_L(y) = y^{\frac{1}{2}} \left\{ 0.4651\, y^2 - 1.1161\, y^3 + 0.6748\, y^4 + 0.1190\, (C_L - 0.1) \right\} .$$

Examples of the total F-function, i.e. $F_L(y) + F_V(y)$, are shown in Fig.16, where the range of y covered was sufficient to make estimates of the front shock wave strengths for each model.

THE PRESSURE SIGNATURE

The static pressure p at any point in the far field, other than at the shock waves, is given by

$$\frac{p - p_o}{p_o} = \frac{\gamma M^2}{\sqrt{2\beta r}} F(y) \qquad (5)$$

where $p_o$ is free-stream static pressure.

The strength of a shock wave is given by

$$\frac{\Delta p}{p_o} = \frac{\gamma M^2}{\sqrt{2\beta r}} \left\{ F(y_1) - F(y_2) \right\} \qquad (6)$$

where $y_1$ and $y_2$ are points behind and ahead of the shock respectively and are defined by the conditions

$$\int_{y_2}^{y_1} F(y)\, dy = \tfrac{1}{2}(y_1 - y_2) \left\{ F(y_1) - F(y_2) \right\}$$

and

$$\frac{F(y_1) - F(y_2)}{y_1 - y_2} = \frac{1}{kr^{\frac{1}{2}}} .$$

In the case of the bow shock wave, $F(y) = 0$ ahead of the shock wave, and equation (6) simplifies to

$$\left(\frac{\Delta p}{p_o}\right)_{\substack{\text{front}\\ \text{shock}}} = \frac{\gamma M^2}{\sqrt{2\beta r}} F(y_1) \qquad (7)$$

where $y_1$ satisfies the condition

$$\frac{\int_o^{y_1} F(y)\, dy}{F^2(y_1)} = \tfrac{1}{2} k r^{\frac{1}{2}} .$$

At very large values of r, it can be shown that the front shock wave strength approaches an asymptotic value, given by:-

$$\left(\frac{\Delta p}{p_o}\right)_{\substack{\text{front}\\ \text{shock}}} = \frac{2^{\frac{1}{4}} \gamma}{(\gamma+1)^{\frac{1}{2}}} \times \frac{\beta^{\frac{1}{4}}}{r^{\frac{3}{4}}} \left\{ \int_o^{y_o} F(y)\, dy \right\}^{\frac{1}{2}} \qquad (8)$$

where $y_o$ corresponds to the first zero of $F(y)$ other than $y = 0$.

The position of either shock wave is given by

$$t = \beta r - G(r) \qquad (9)$$

where $G(r) = k F(y_1) r^{\frac{1}{2}} - y_1$, for the front shock wave,

and $G(r) = k F(y_1) r^{\frac{1}{2}} - y_1$,
$= k F(y_2) r^{\frac{1}{2}} - y_2$, } for the rear shock wave.

For the present models, the measuring station was not sufficiently far from the models to justify the use of equation (8) for accurate estimates of front shock wave strengths, as is apparent from Fig. 13. These have therefore been made using equation (7), and the complete pressure signature for Models A and B at $C_L = 0$ has been estimated (Fig. 10) using equations (5), (6), (7) and (9).

---

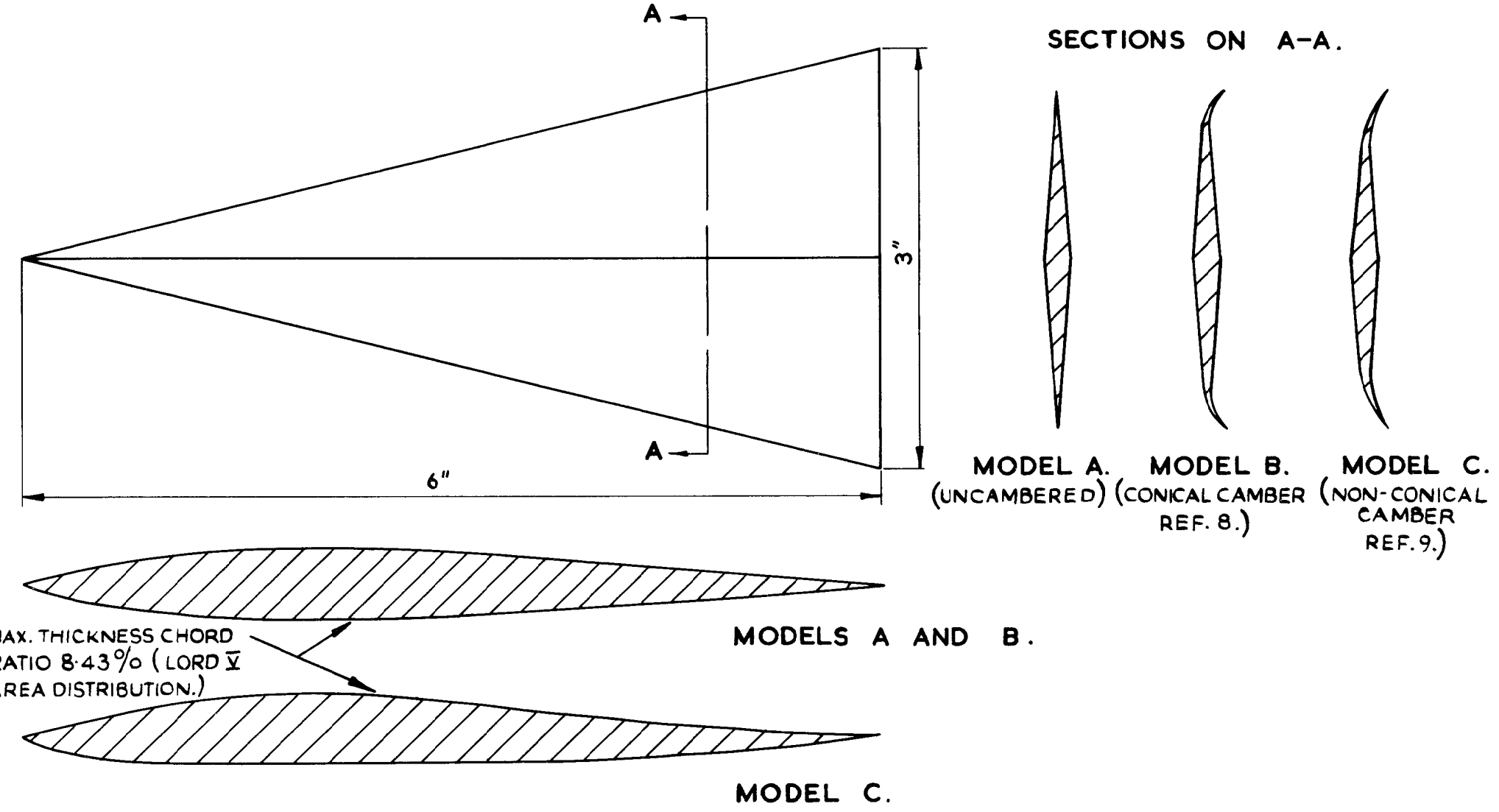


FIG. 1. DETAILS OF MODELS A, B AND C.

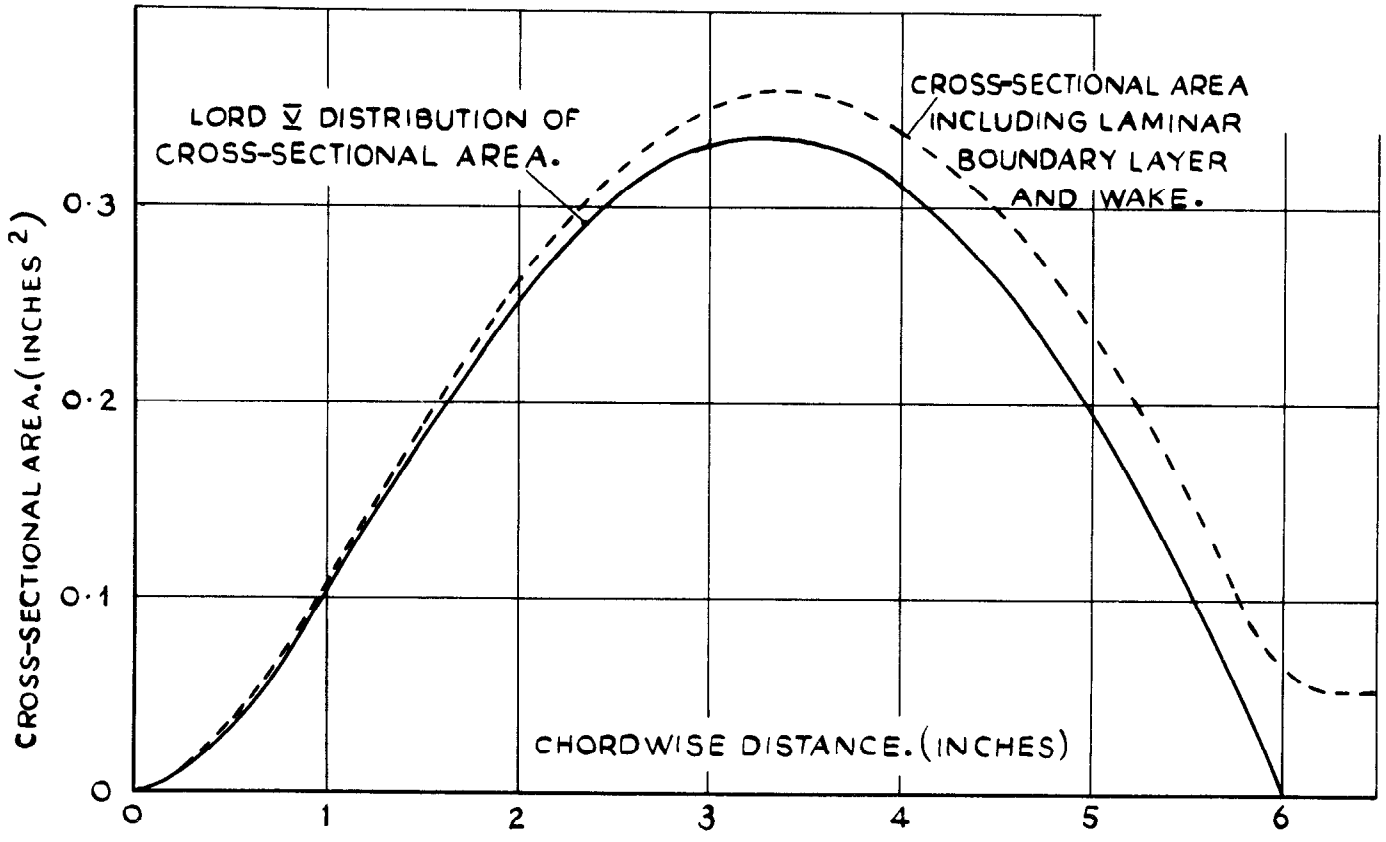


FIG. 2. LENGTHWISE DISTRIBUTION OF CROSS-SECTIONAL AREA OF THE MODELS.

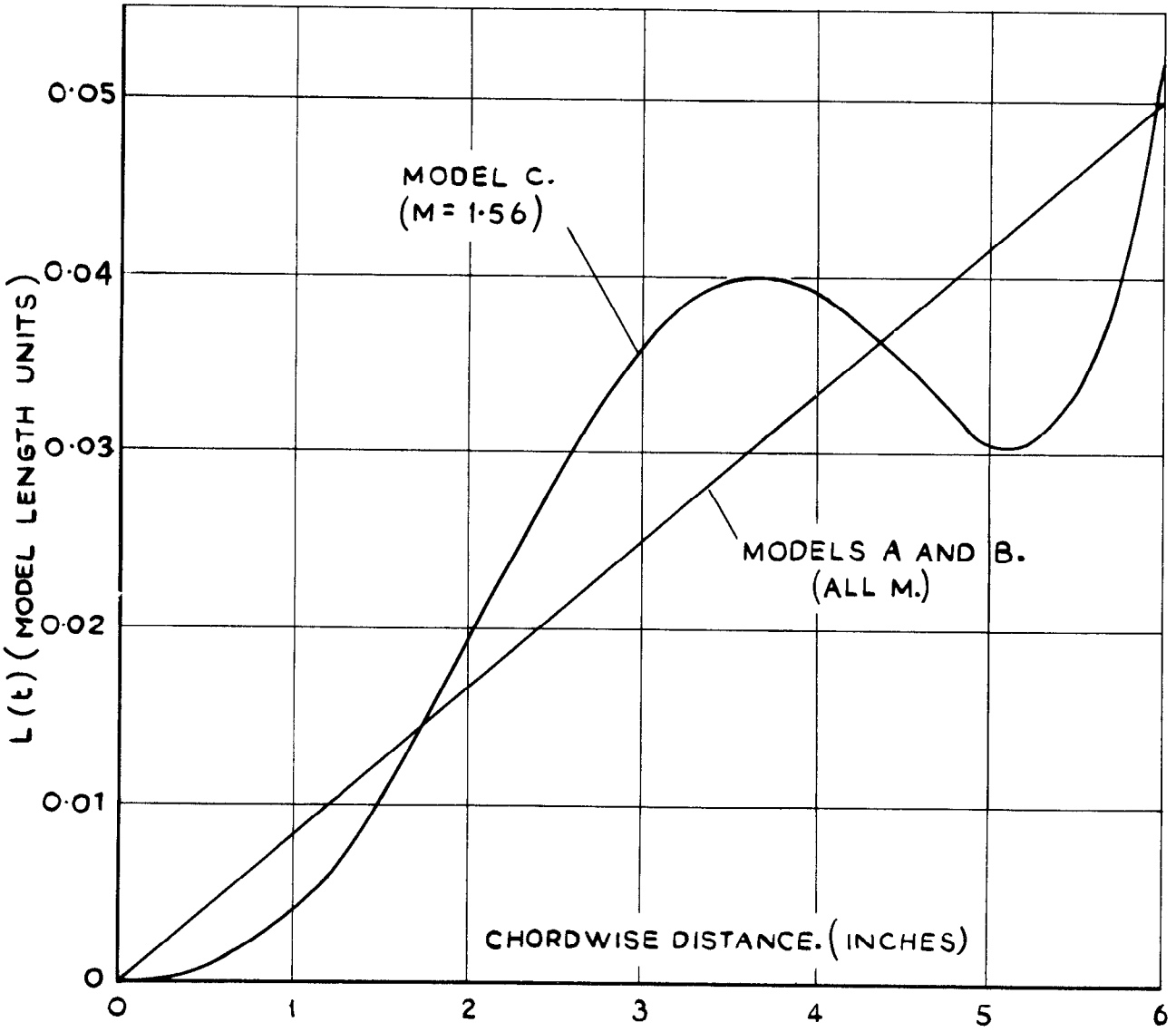


FIG. 3. LENGTHWISE DISTRIBUTION OF LIFT ON THE MODELS AT $C_L = 0{\cdot}1$.

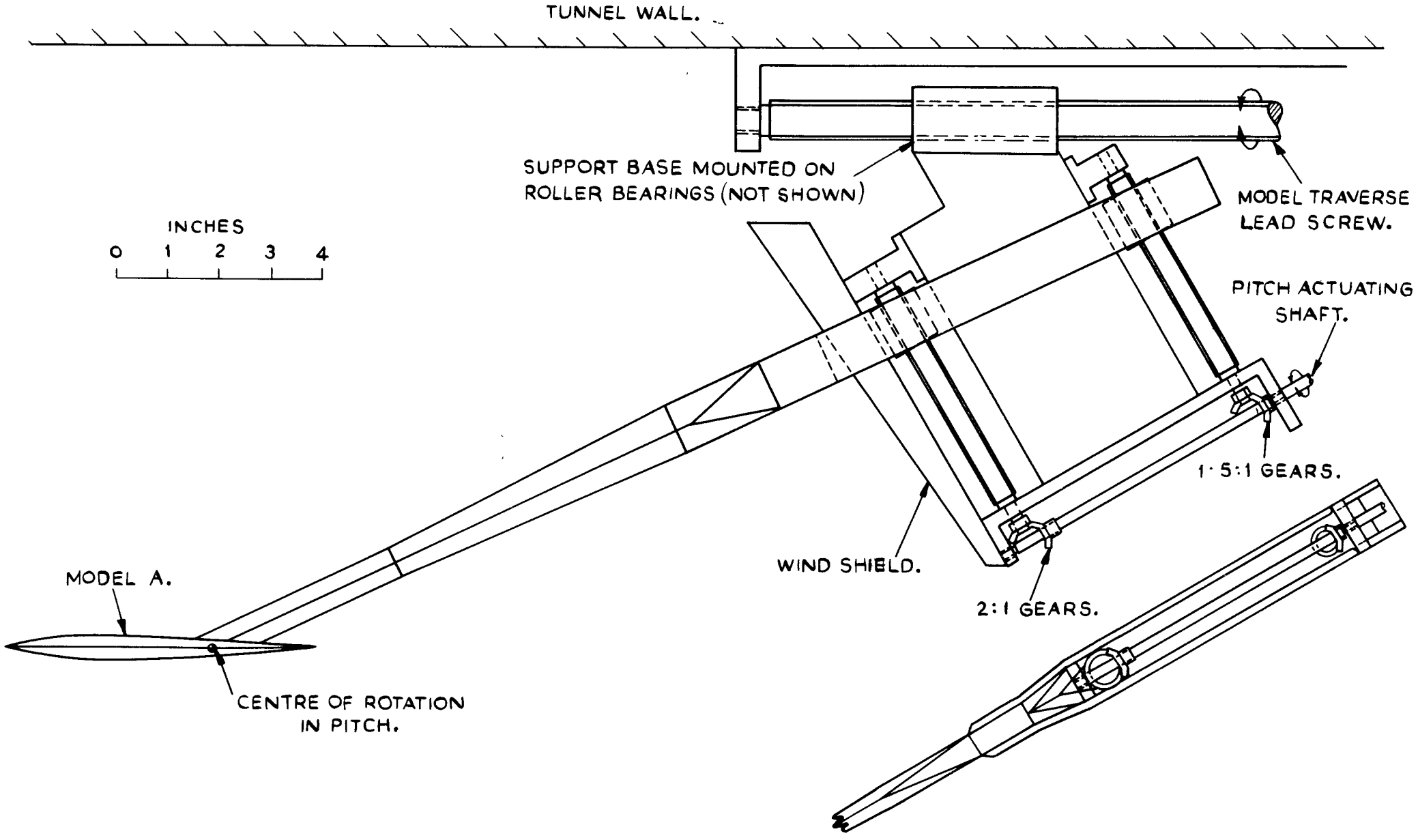


FIG. 4. SKETCH OF MODEL SUPPORT AND ACTUATING SYSTEM.

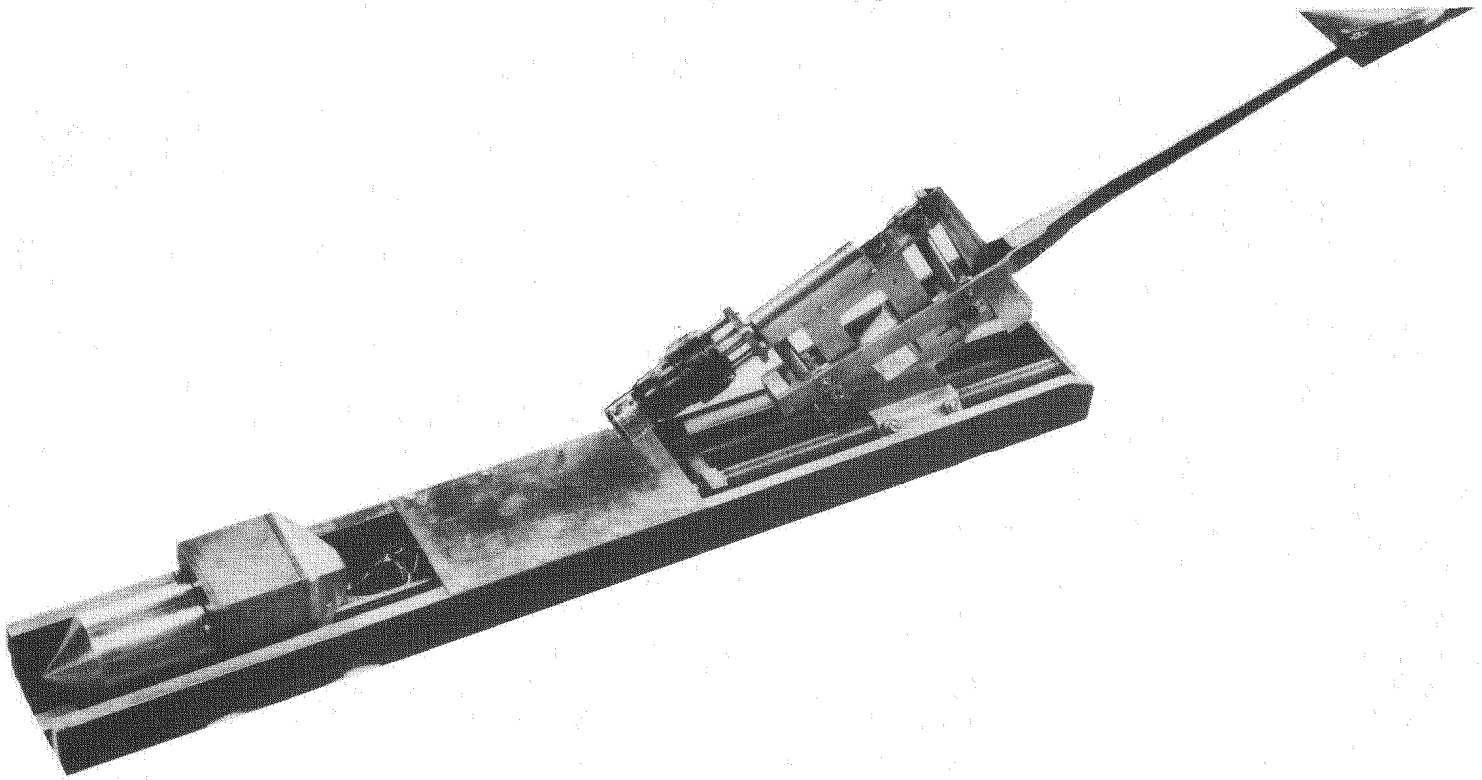

FIG.5. MODEL ON THE SUPPORT SYSTEM

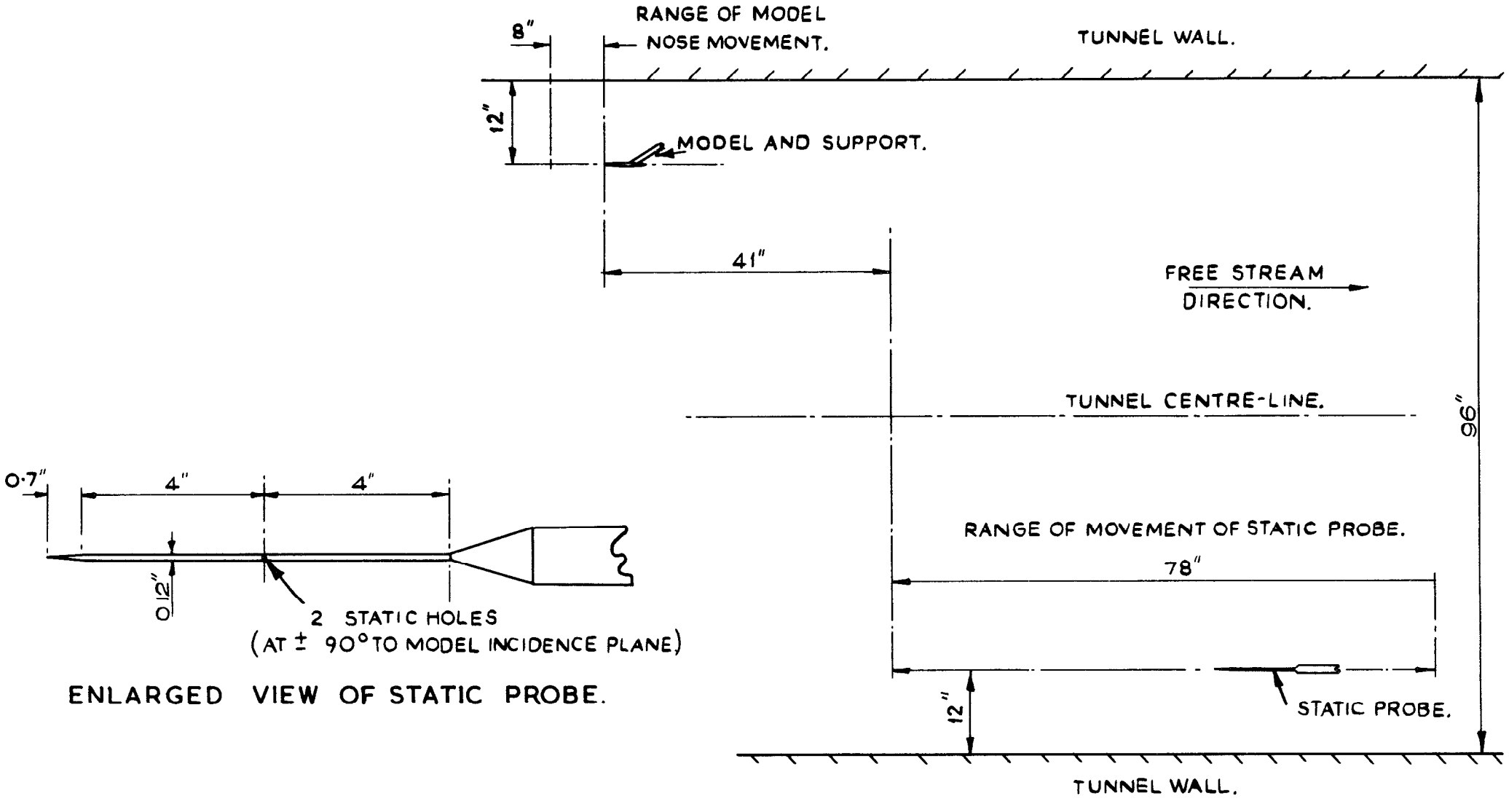


FIG. 6. ARRANGEMENT OF MODEL AND PROBE IN THE WIND TUNNEL.

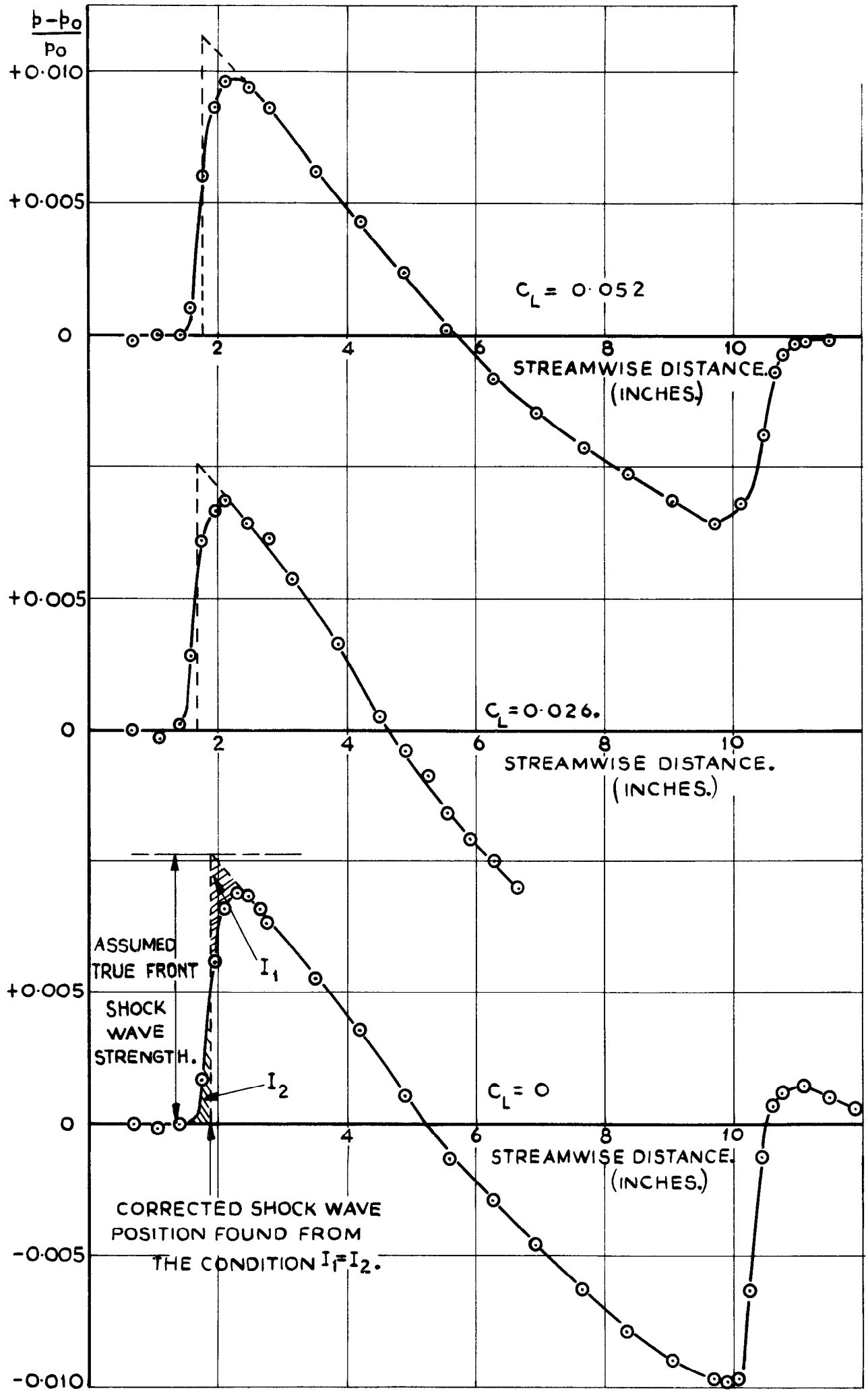


FIG. 7. PRESSURE MEASUREMENTS FOR MODEL A.

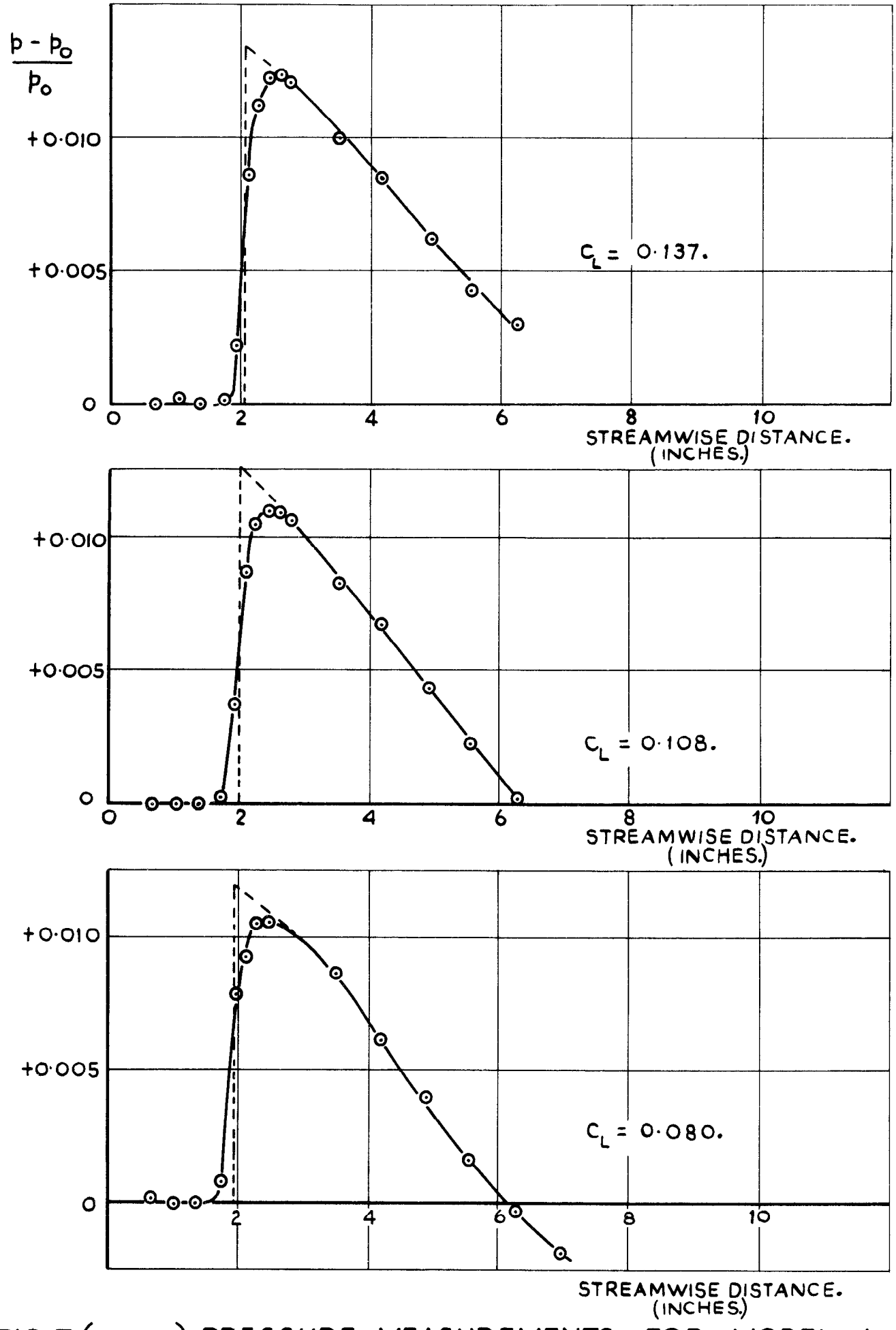


FIG. 7.(CONTD.) PRESSURE MEASUREMENTS FOR MODEL A.

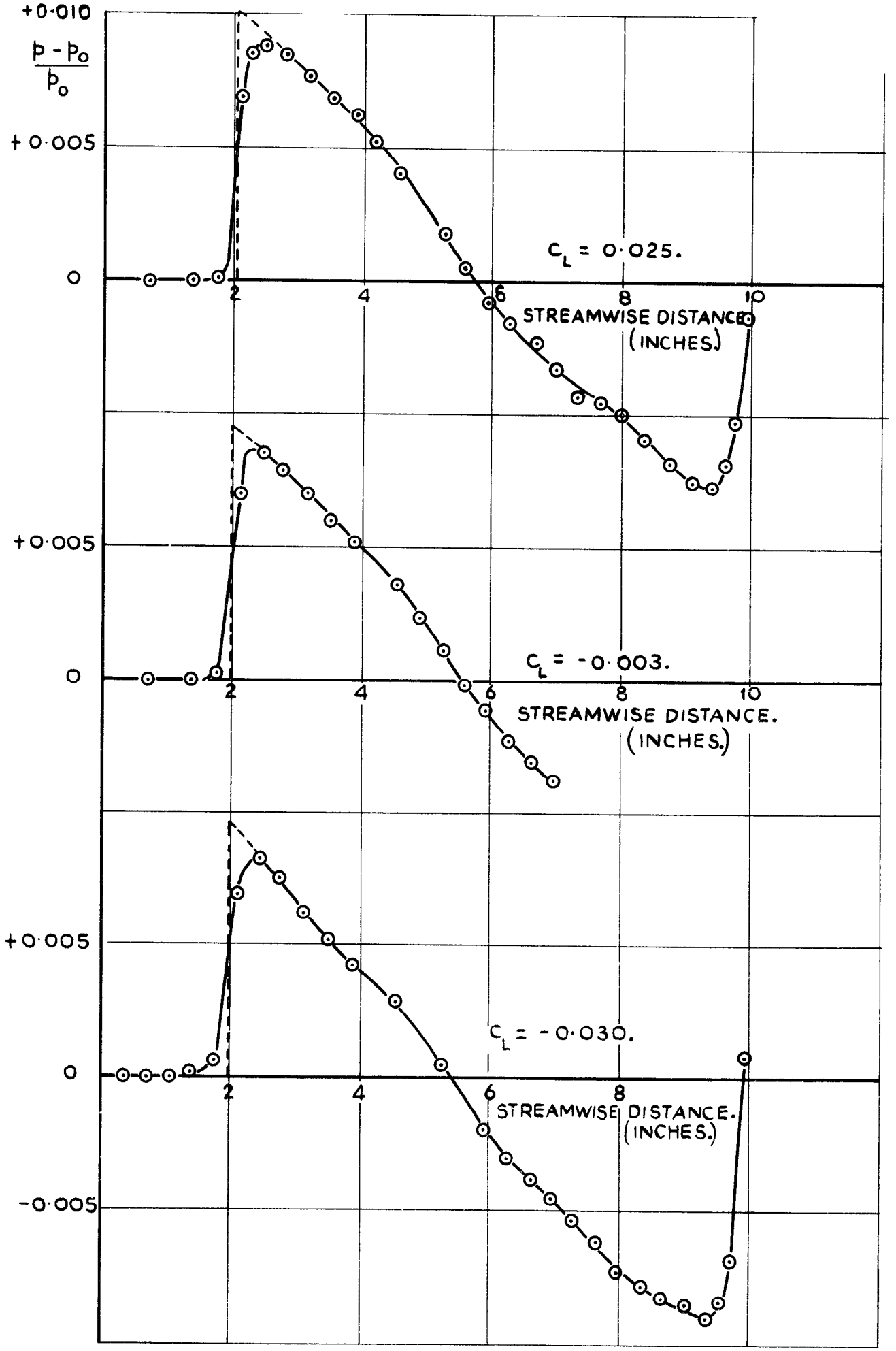


FIG. 8. PRESSURE MEASUREMENTS FOR MODEL B.

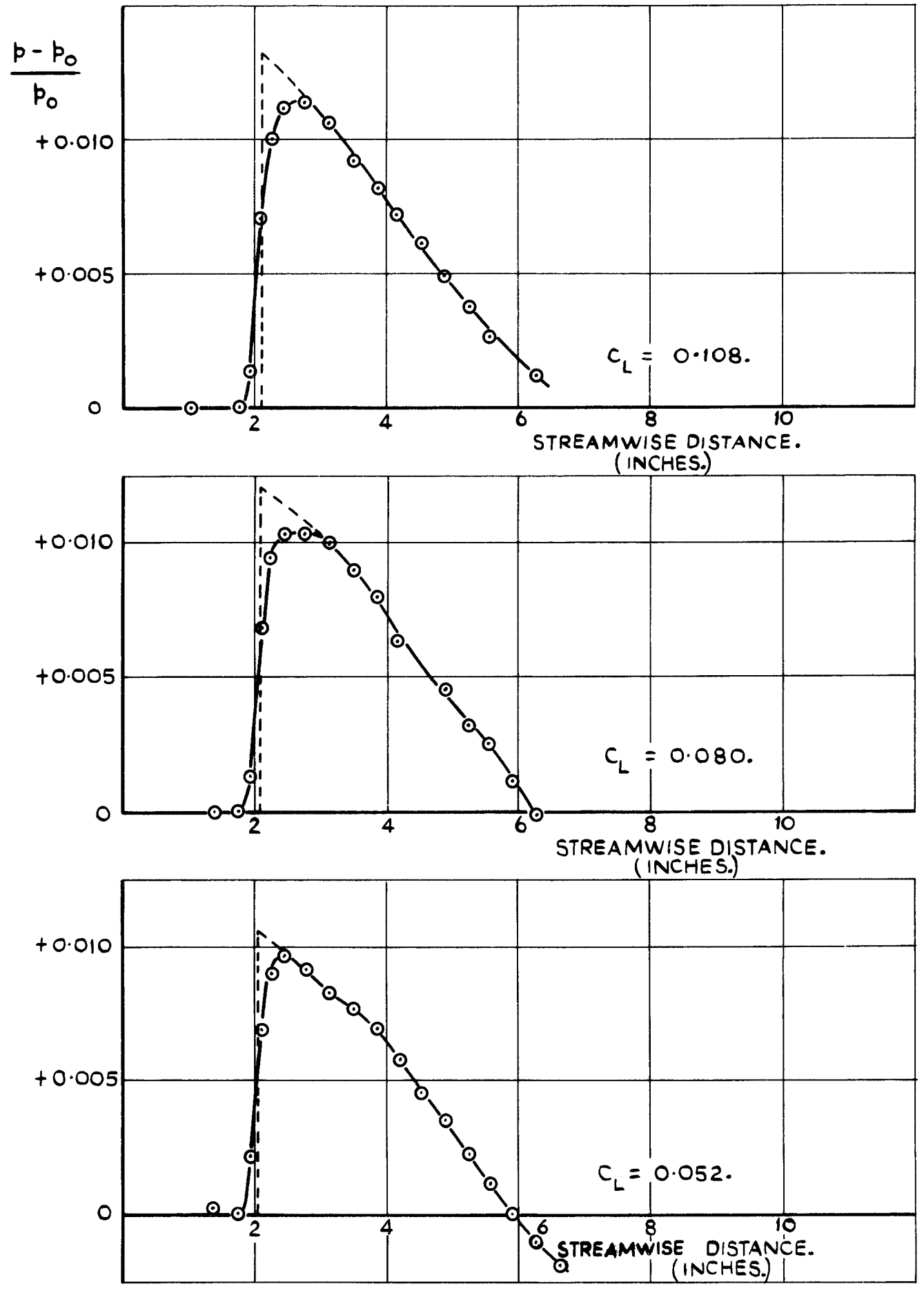


FIG. 8.(CONTD.) PRESSURE MEASUREMENTS FOR MODEL B.

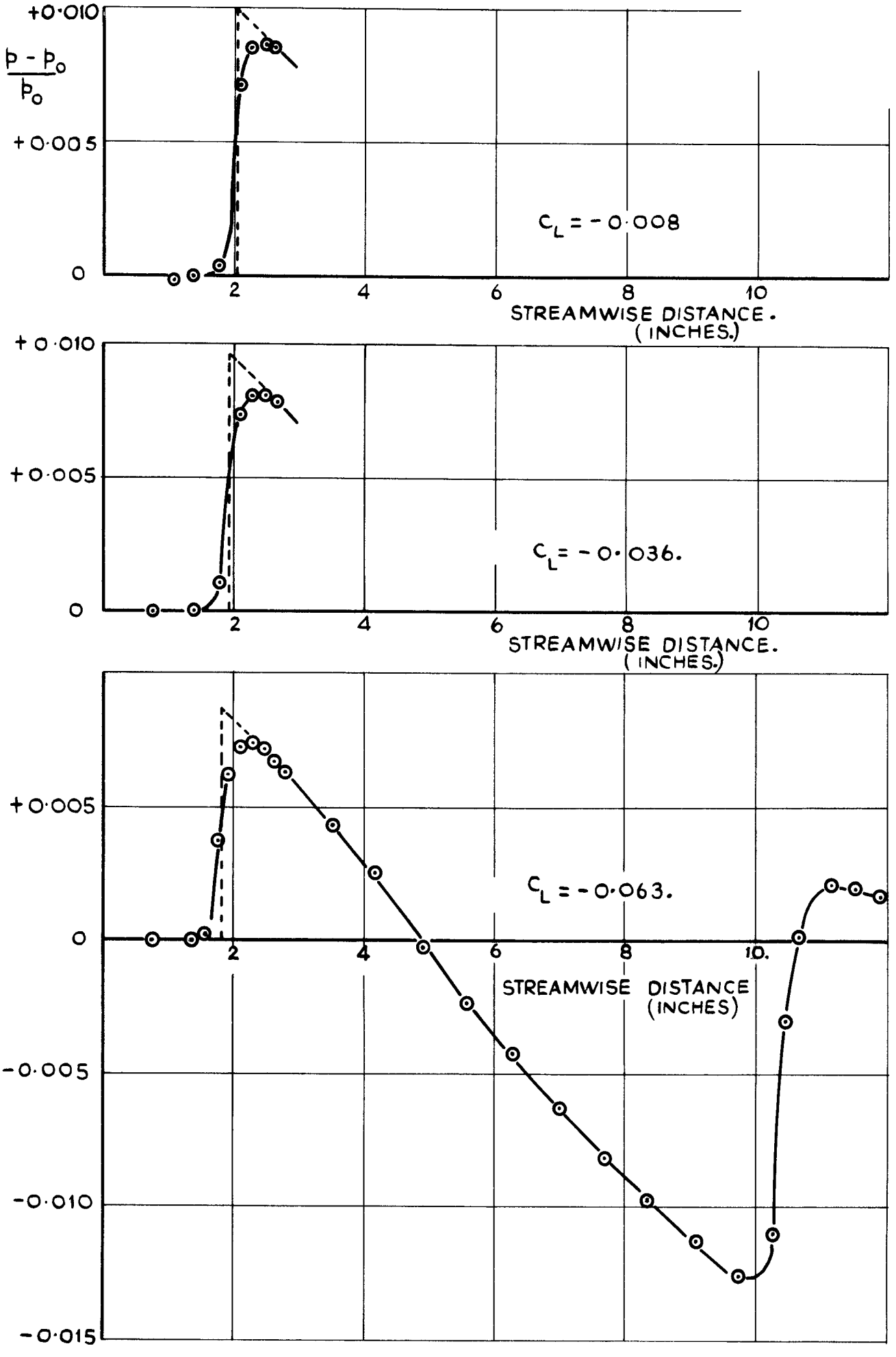


FIG. 9. PRESSURE MEASUREMENTS FOR MODEL C.

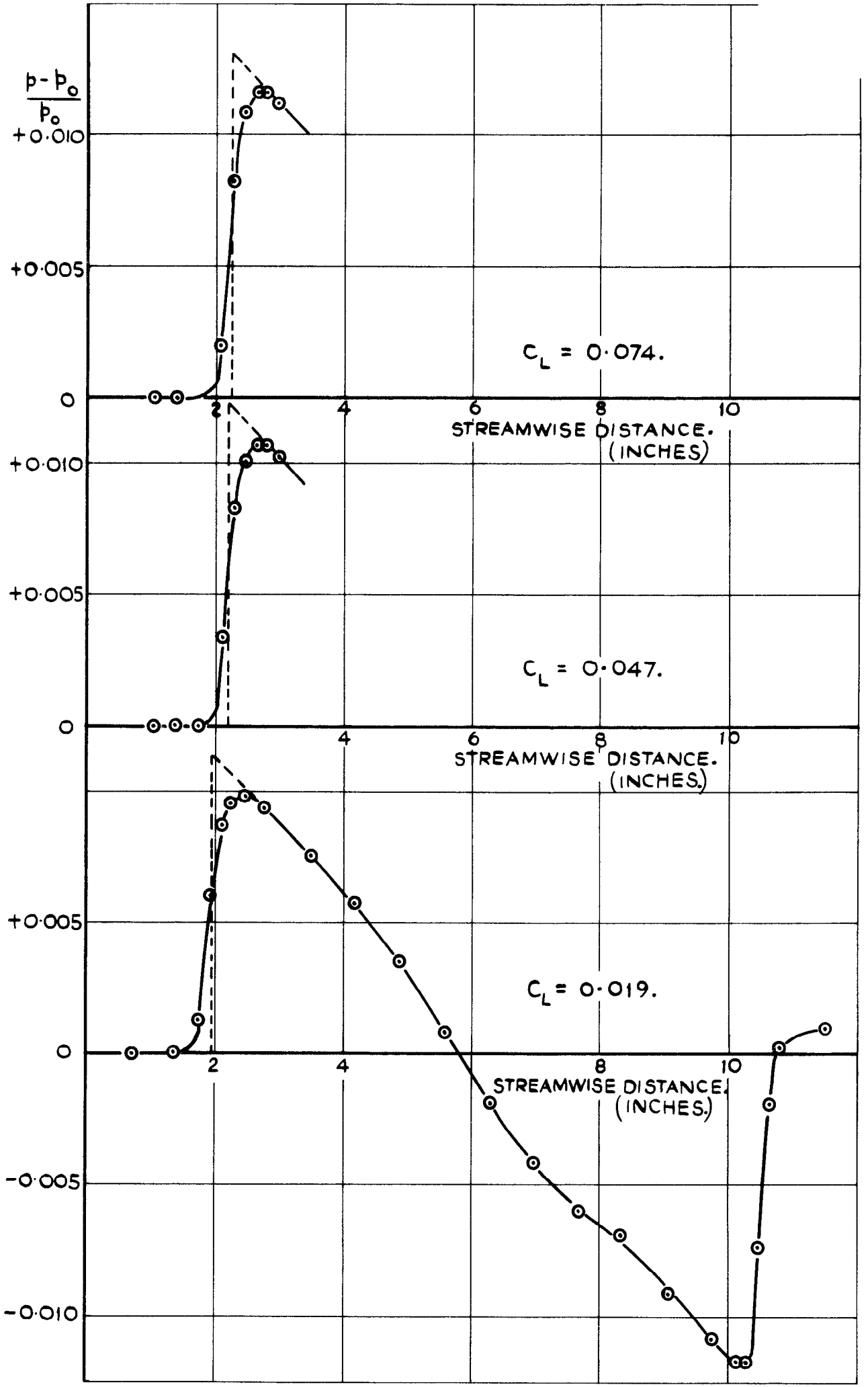


FIG. 9. (CONTD.) PRESSURE MEASUREMENTS FOR MODEL C.

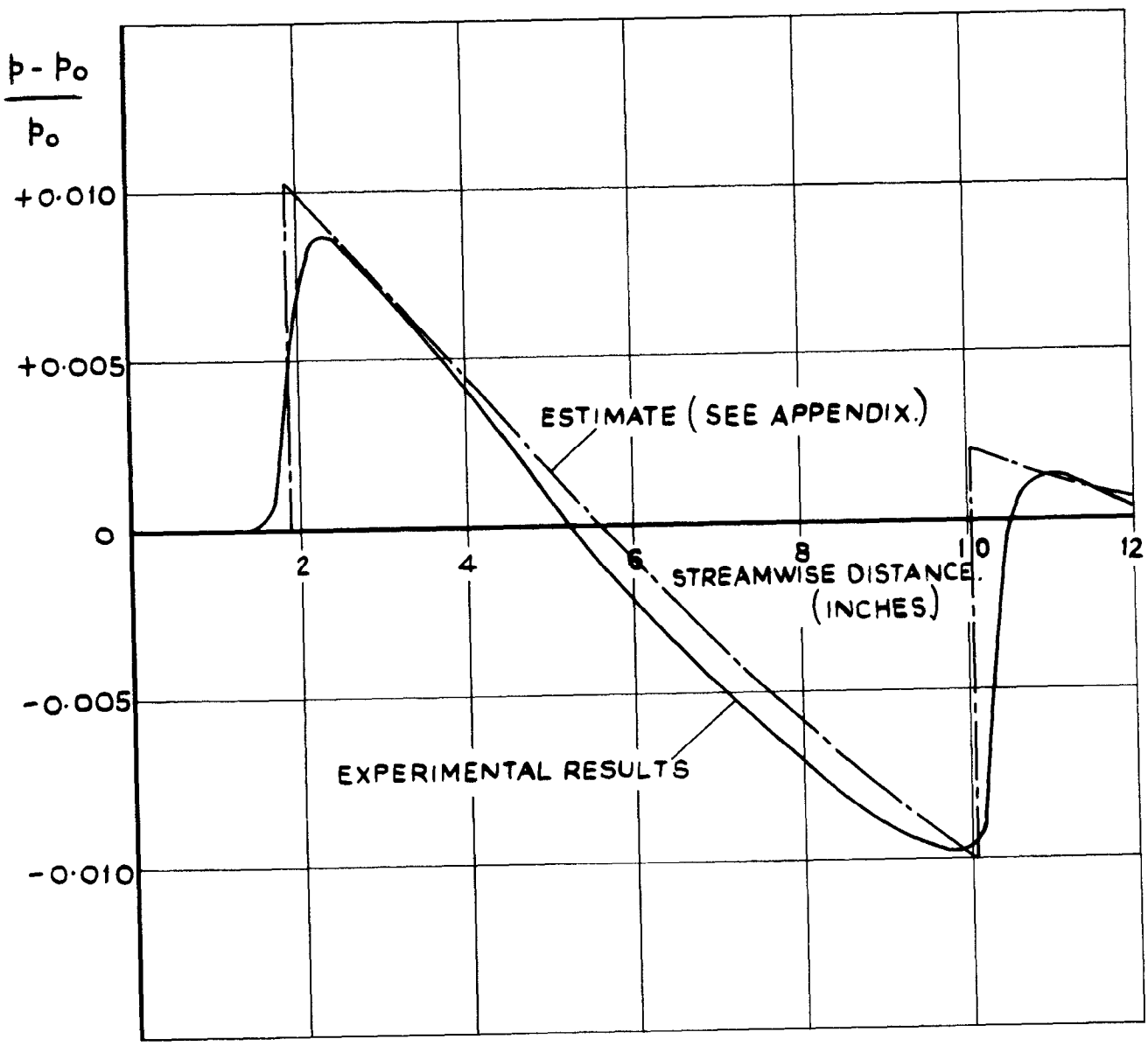


FIG. 10. COMPARISON OF EXPERIMENTAL AND ESTIMATED PRESSURE SIGNATURES FOR MODEL A AT $C_L = 0$.

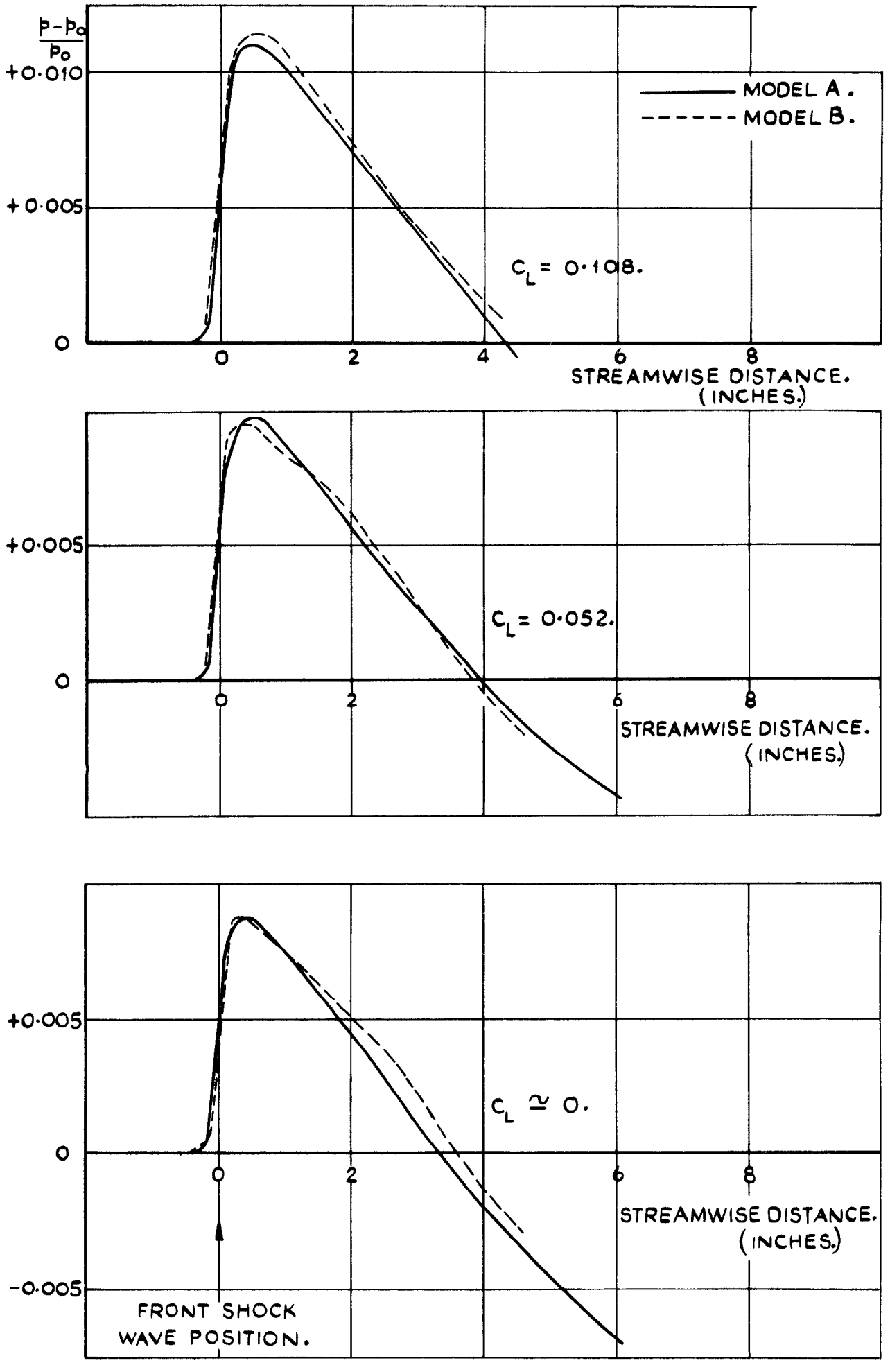


FIG. 11. COMPARISON OF PRESSURE MEASUREMENTS FOR MODELS A AND B.

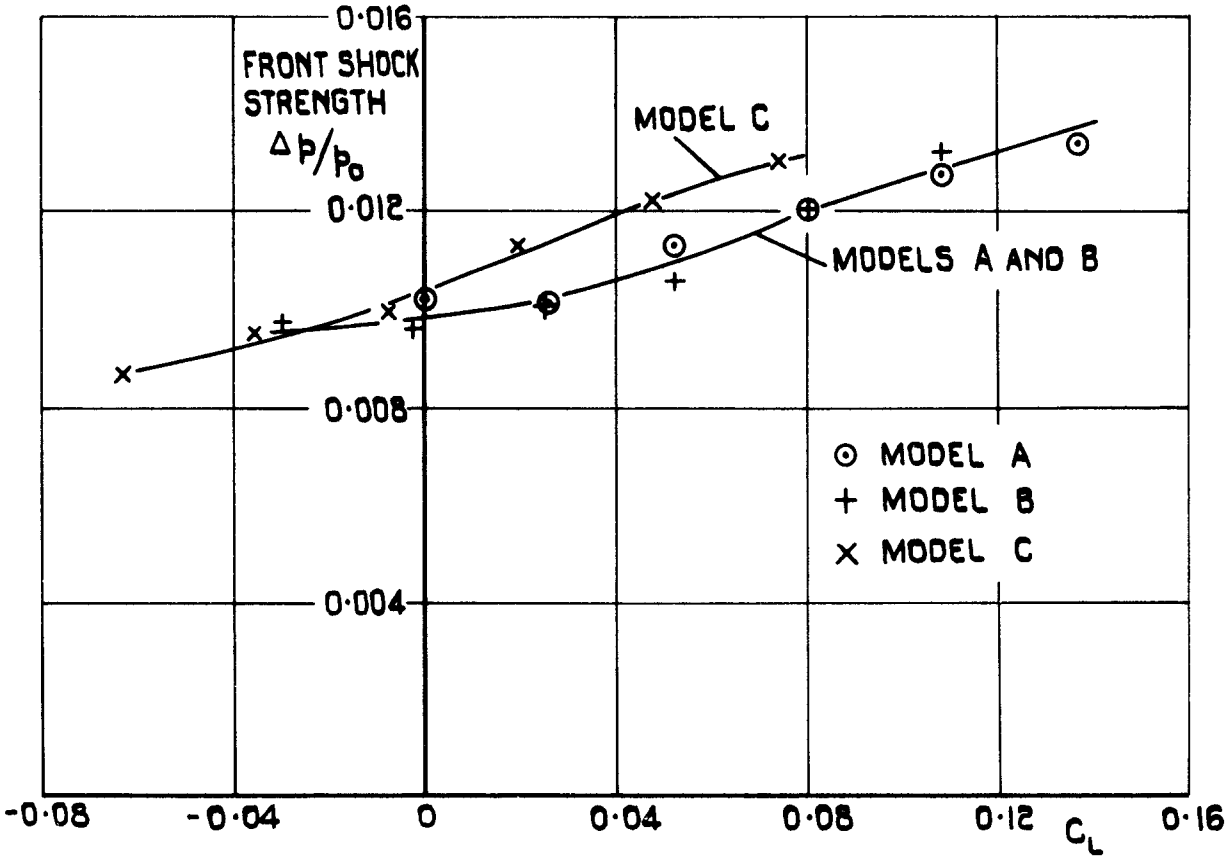


FIG. 12. MEASURED FRONT SHOCK STRENGTHS OF MODELS A, B AND C.

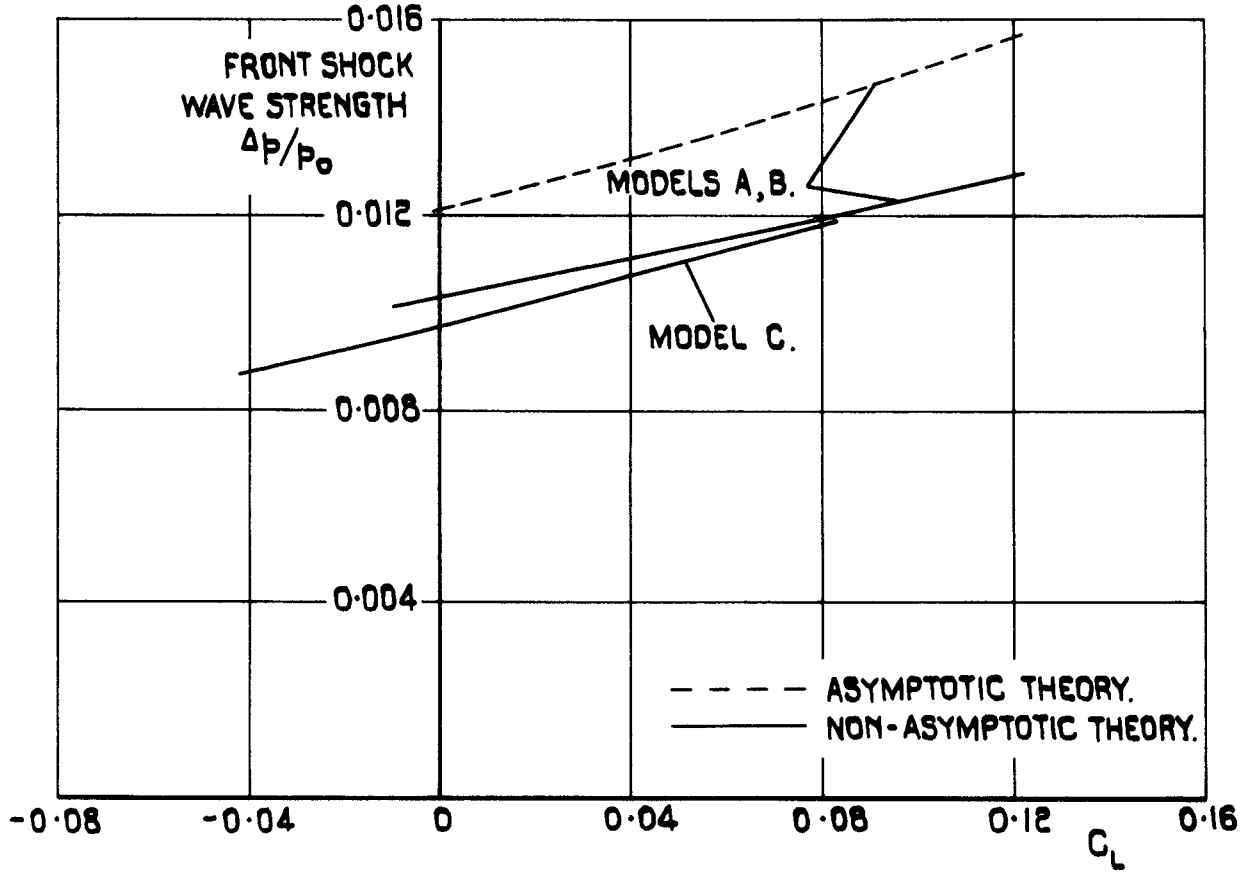


FIG. 13. ESTIMATED FRONT SHOCK STRENGTHS OF MODELS A, B AND C.

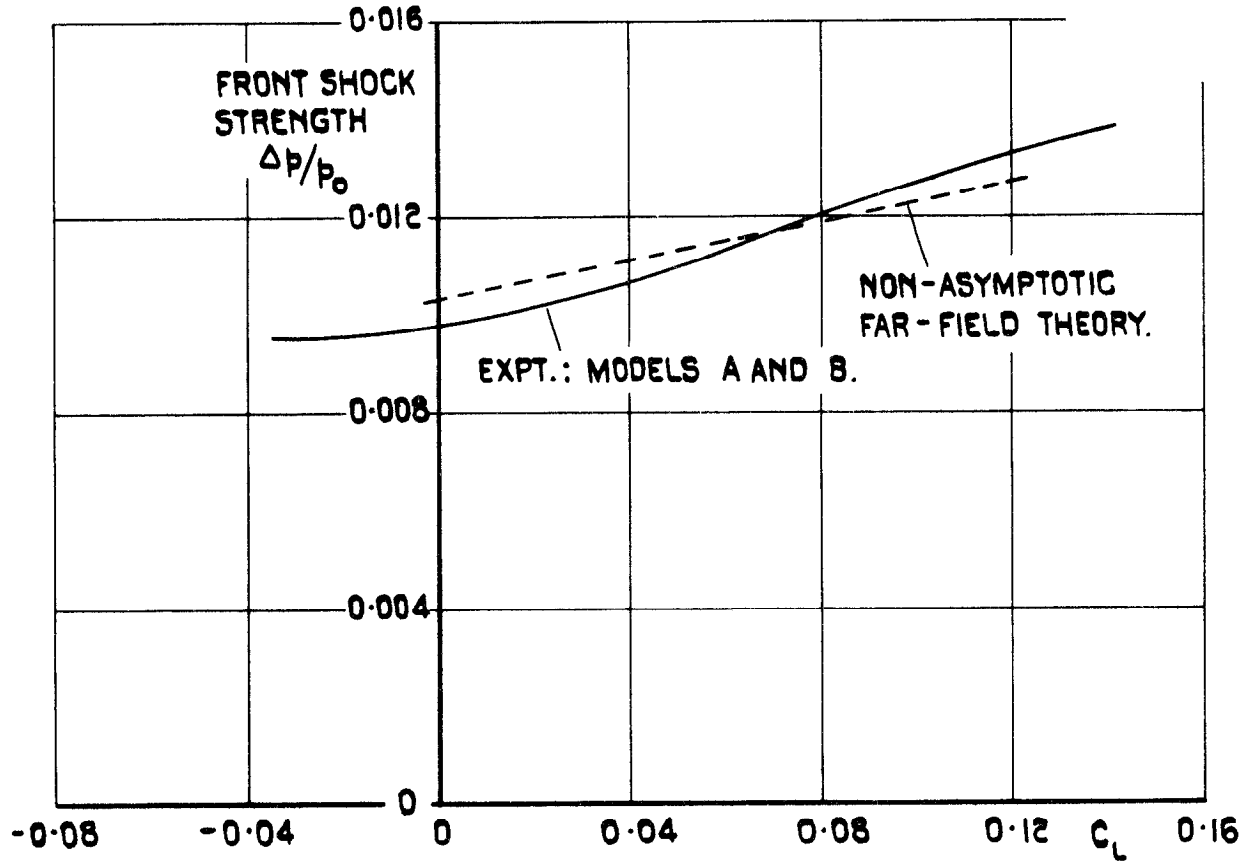


FIG. 14. COMPARISON OF MEASURED AND ESTIMATED FRONT SHOCK STRENGTHS FOR MODELS WITH CONICAL LIFT DISTRIBUTION.

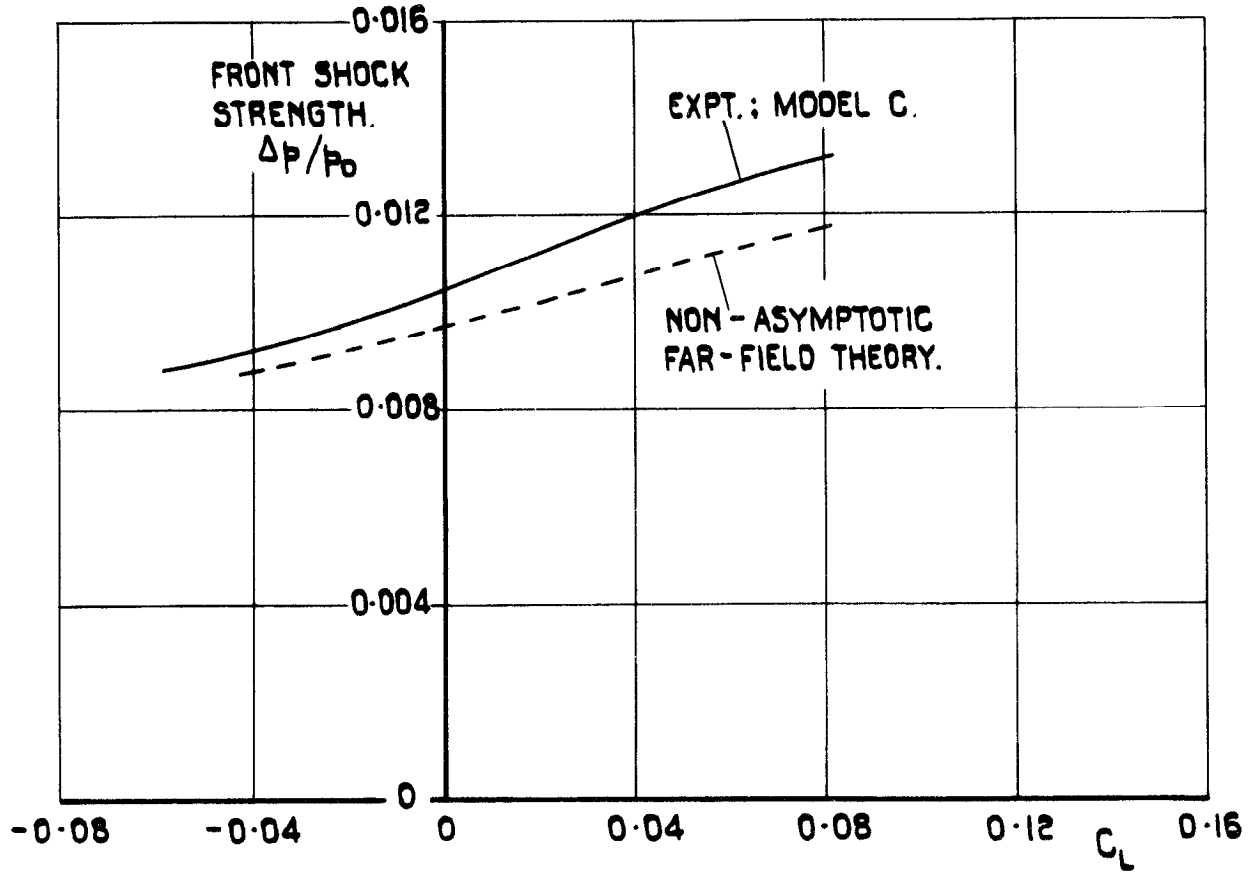


FIG. 15. COMPARISON OF MEASURED AND ESTIMATED FRONT SHOCK STRENGTHS FOR MODEL WITH NON-CONICAL LIFT DISTRIBUTION.

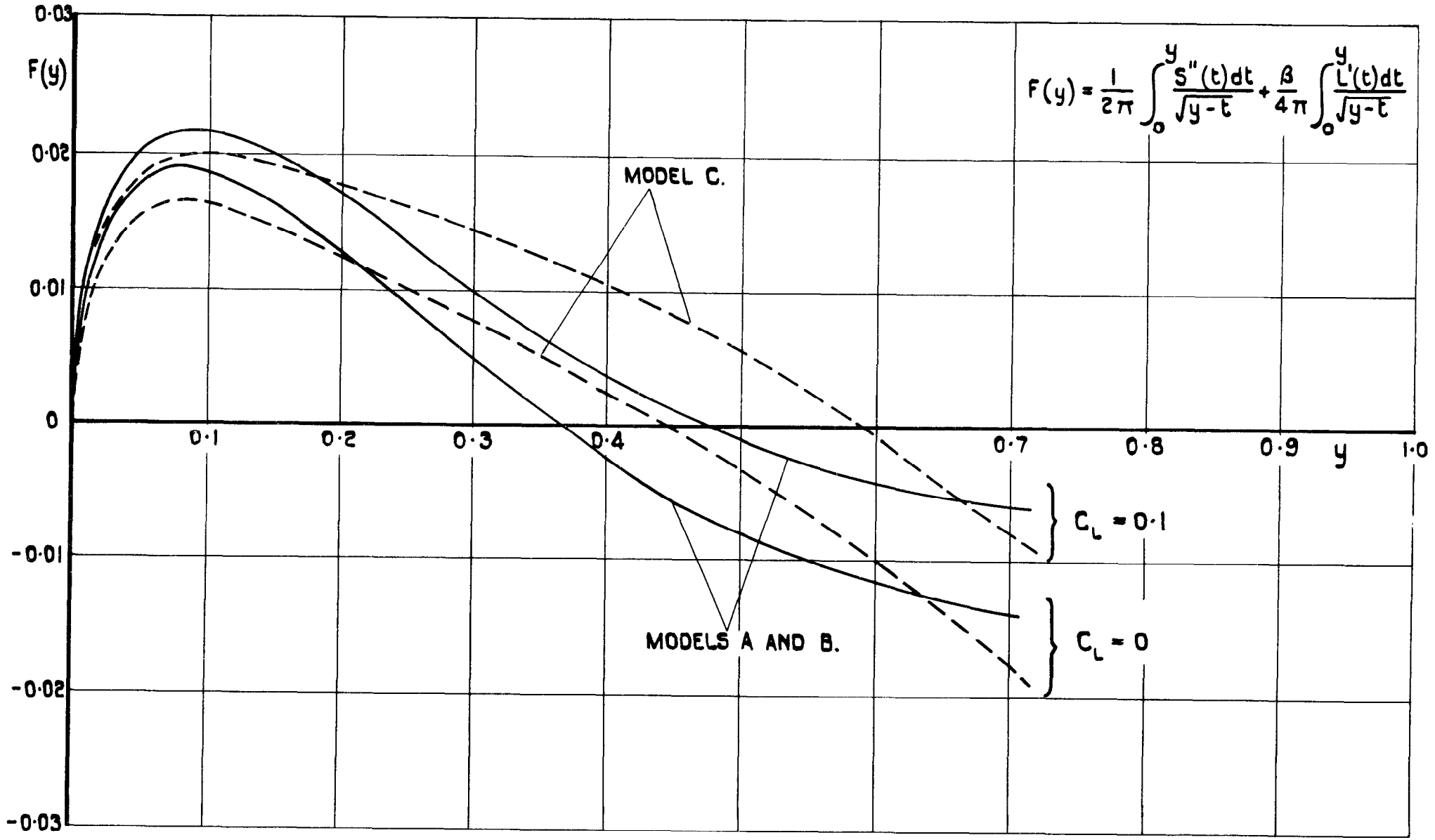


FIG. 16. TYPICAL F-FUNCTIONS USED TO ESTIMATE FRONT SHOCK WAVE STRENGTHS.

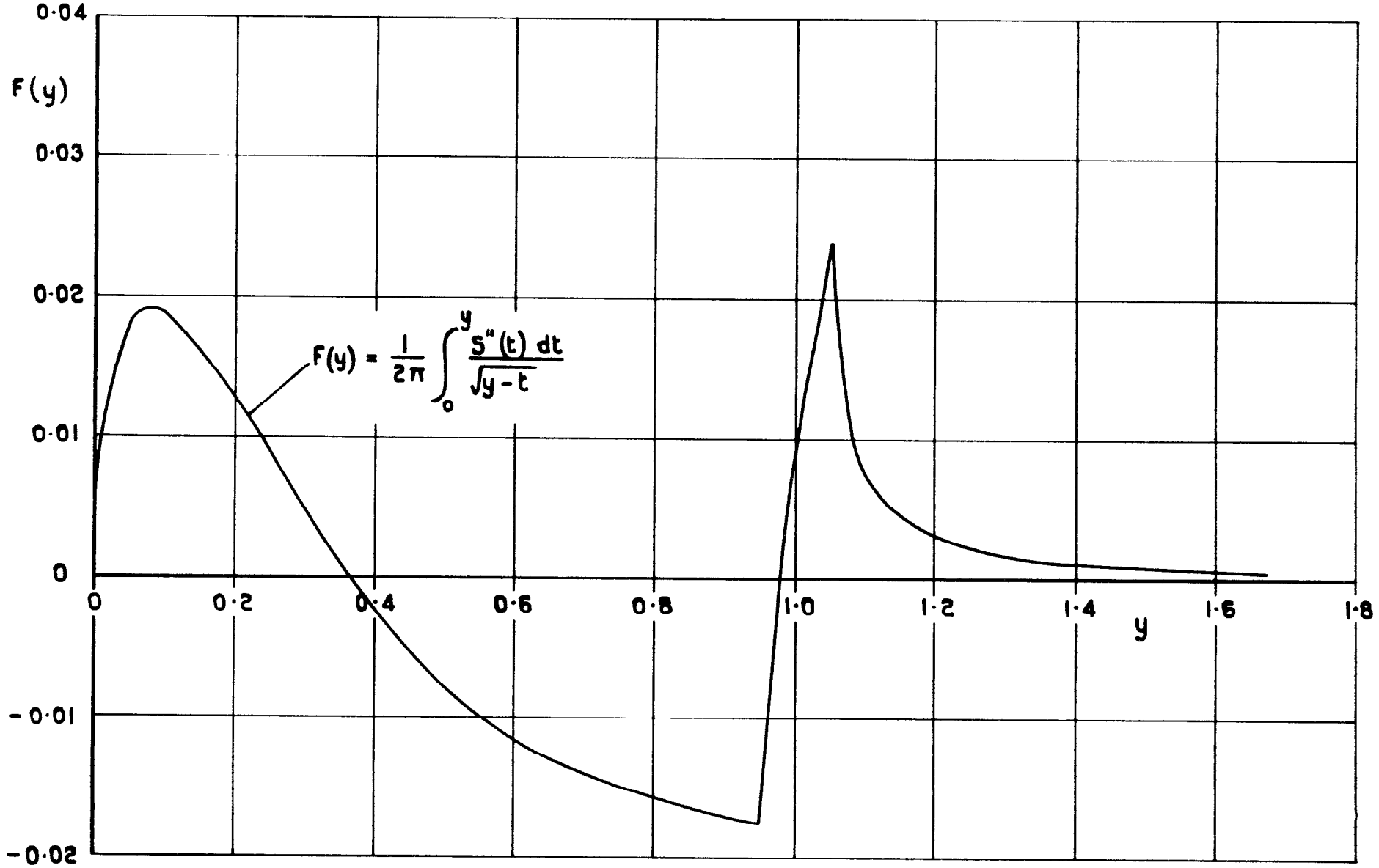


FIG. 17. COMPLETE F-FUNCTION FOR MODELS A AND B AT ZERO $C_L$.

*Printed in England for Her Majesty's Stationery Office by the Royal Aircraft Establishment, Farnborough. W.T.60. K.4.*

A.R.C. C.P. No. 802

533.693.3 :
533.6.048.2 :
533.6.011.5

WIND TUNNEL MEASUREMENTS OF THE FAR-FIELD PRESSURES DUE TO SOME LIFTING, SLENDER DELTA WINGS. Cook, T.A. August, 1964.

Measurements have been made of the pressure field in the plane of symmetry of each of three slender delta wings of unit aspect ratio, at a distance of 12 model lengths from each model and at a Mach number of 1.80. One model was uncambered while the others were cambered to have attached flow at their leading edges at $C_L = 0.1$: the cambered models had different lengthwise lift distributions.

Estimates of the front shock wave strengths of the models made using Whitham's theory were found to be in good agreement with the measured values, though estimates of lift effects seemed a little low. An estimate of the complete pressure signature of a model at zero lift agreed well with measurements.

A.R.C. C.P. No. 802

533.693.3 :
533.6.048.2 :
533.6.011.5

WIND TUNNEL MEASUREMENTS OF THE FAR-FIELD PRESSURES DUE TO SOME LIFTING, SLENDER DELTA WINGS. Cook, T.A. August, 1964.

Measurements have been made of the pressure field in the plane of symmetry of each of three slender delta wings of unit aspect ratio, at a distance of 12 model lengths from each model and at a Mach number of 1.80. One model was uncambered while the others were cambered to have attached flow at their leading edges at $C_L = 0.1$: the cambered models had different lengthwise lift distributions.

Estimates of the front shock wave strengths of the models made using Whitham's theory were found to be in good agreement with the measured values, though estimates of lift effects seemed a little low. An estimate of the complete pressure signature of a model at zero lift agreed well with measurements.

A.R.C. C.P. No. 802

533.693.3 :
533.6.048.2 :
533.6.011.5

WIND TUNNEL MEASUREMENTS OF THE FAR-FIELD PRESSURES DUE TO SOME LIFTING, SLENDER DELTA WINGS. Cook, T.A. August, 1964..

Measurements have been made of the pressure field in the plane of symmetry of each of three slender delta wings of unit aspect ratio, at a distance of 12 model lengths from each model and at a Mach number of 1.80. One model was uncambered while the others were cambered to have attached flow at their leading edges at $C_L = 0.1$: the cambered models had different lengthwise lift distributions.

Estimates of the front shock wave strengths of the models made using Whitham's theory were found to be in good agreement with the measured values, though estimates of lift effects seemed a little low. An estimate of the complete pressure signature of a model at zero lift agreed well with measurements.

**Published by**
HER MAJESTY'S STATIONERY OFFICE

To be purchased from
York House, Kingsway, London W.C.2
423 Oxford Street, London W.1
13A Castle Street, Edinburgh 2
109 St. Mary Street, Cardiff
39 King Street, Manchester 2
50 Fairfax Street, Bristol 1
35 Smallbrook, Ringway, Birmingham 5
80 Chichester Street, Belfast 1
or through any bookseller

C.P. No. 802

S.O. CODE No. 23-9016-2